DROP TEST DESCRIPTION AND EVALUATION OF A LANDING LEG FOR A RESUSABLE FUTURE LAUNCH VEHICLE

Author: Christoph Thies

MT Aerospace AG, Franz-Josef-Strauß-Straße 5, D-86153 Augsburg, Germany
christoph.thies@mt-aerospace.de

ABSTRACT

The RETALT project, funded by the European Horizon 2020 program, has the objective to study critical technologies for Vertical Take-off Vertical Landing (VTVL) Reusable Launch Vehicles (RLVs) applying retro propulsion, combined with aerodynamic control surfaces and landing gear components. Two reference launch vehicle configurations are defined:

RETALT1, which is a Two Stage To Orbit (TSTO) RLV similar to the SpaceX rocket "Falcon 9" and RETALT2, which is a Single Stage To Orbit (SSTO) RLV similar to the DC-X vehicle.

This paper describes a scaled drop test procedure for a scaled landing leg 1:5 (LL) of the reusable launcher configuration RETALT1 and summarizes the recorded data of the performed short time dynamic impact test.

The performed drop test simulates a dynamic shock loading (landing manoeuvre) on the 1:5 scaled landing structure to proof the strength resistance of the frames during landing. Additionally, the functionality of the kinematic system and the resistance and damping behaviour of the absorber is tested. The test results are used to correlate the mathematical strength and kinetic models for future works and provide an upscale methodology to the 1:1 launcher configuration for the landing gear.

The drop test consists of a large mass, which is mounted on a drop tower to store high potential energy, which is then transformed into kinetic energy after the release of the mass. After touching the foot pad of the LL, the impact energy leads to high forces in the landing leg and absorber. To withstand the applied kinetic energy, the compression and tension forces in the lightweight carbon fibre reinforced polymer (CFRP) LL were simulated via FEM. The applied kinetic energy quantity matches the optimal efficiency range of the non-linear damper system.

During the drop test the landing gear is equipped with high sampling accelerometers, strain gauges and an optical measurement system for the detection of the deformation and strains at critical positions such as interfaces, hinges, rivets and highly stressed CFRP components.

Furthermore, a short description of the control fins is represented in this paper, which were built by MT-Aerospace (MTA) and used for the development of kinematic mechanisms by MTA's partner Almatech.

Index terms: Reusable launch vehicle, landing leg, impact loads, drop test experiment, test evaluation, FEM, control fins

Acronyms/Abbreviations

ACS	Aerodynamic Control Surface
CFRP	Carbon Fibre Reinforced Polymer
CoG	Centre of Gravity
DMS	Dehnmessstreifen
ECSS	European Cooperation for Space Standardization
EM	Engineering Model
ESA	European space Agency
FEM	Finite Element Method
I/F	Interface
IFF	Inter Fibre Failure
LL	Landing Leg
MAM	Metallic Additive Manufacture
MBD	Multi Body Dynamics
MoS	Margin of Safety
MTA	MT Aerospace
QSL	Quasi Static Loading
RETALT	Retro Propulsion Assistant Landing
RLV	Reusable Launch Vehicle
RT	Room Temperature
S/C	Spacecraft
SSTO	Single Stage To Orbit
Ti	Titanium
TRL	Test Readiness Level
TSTO	Two Stage To Orbit
VTVL	Vertical Take-off Vertical Landing

1   INTRODUCTION

After approximately 3.5 years of development, MTA will complete successfully the so-called RETALT programme in August the 31th in 2022 in Brussels. MTA contributed two prototype structures for reusable space vehicle applications for this in 2 phases structured programme for MTA. During the first phase, a control fin was designed and manufactured and subsequently provided to the partner Almatech for functional mechanism testing. During the second phase, the second structure, the LL was manufactured and tested by MTA concerning its functionality and strength resistance.

The LL represents a first approach for a lightweight landing gear for reusable launchers. After the development of the LL, MTA completed successfully the test campaign for the landing leg in 2022 in the Leichtbau Zentrum Sachsen (LZS).

The LL, designed mainly as a CFRP structure including additional high strength metallic components, serves as key element for a new-generation of reusable launchers.

Within the scope of the development efforts, main support structures are built in 1:5 scaling and covering structures for aerodynamic applications are implemented on the load carrying frames.

Three main components (LL, absorber/ absorber rod, massive test rig see. Figure 2-3) had to be delivered to the test facility to conduct the functional and stress resistance test. The paper focuses in detail on the LL and the corresponding test. This includes the test description, test evaluation and kinetic/ structural investigation of a scaled 1:5 LL during landing, simulated by an impact test. The test serves to proof the kinematic functionality of the LL and to study the structural dynamic behaviour. It also serves to generate a database to correlate the FEM predictions of the strength analysis with the test and the elasto-kinematics for future investigations.

The paper is laid out as follows:

The section 1 gives an overview of the paper in general and explains the intention of test campaign.

Section 2 describes the design such as the geometry, materials and mass of the 1:1 full-scale and the 1:5 scaled test breadboard. Section 3 describes the test campaign including the main objectives, the test description, the test matrix, the test results and the short summary of the evaluation of the test results. Section 4 describes briefly the fins. A detailed description of the control fins is given in the document [3]. The final section 5 draws a conclusion and an outlook of future work is given.

2   GEOMETRY AND DESIGN

In this chapter the geometry of the LL is represented, including the size and the mass. The main components and the applied materials are shortly summarized and explained.

2.1   Geometry of test breadboard

The geometry of the 1:5 scaled test breadboard is based on the 1:1 landing leg configuration of the RETALT1 launcher in the deployed configuration (see

Figure 2-1). The need of scaling was resulting from the following reasons:

- space limitation of the test facility to apply impact loading
- financial reasons of the limited budget within the RETALT project for manufacturing processes e.g. metallic tools for the CFRP, cost of base materials such as Ti-6-4

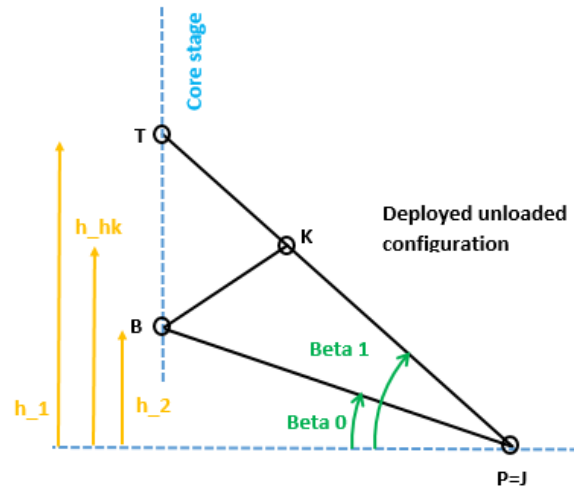The dimensions of the 1:1 and scaled 1:5 landing leg is given in Table 2-1.

Figure 2-1: Overview of geometric parameters of the landing gear in deployed configuration

Name	Abb.	1:1 model	1:5 model
Height of upper attach. T from ground [m]	h_1	8.86	1.77
Height of upper attach. K from ground [m]	h_hk	6.03	1.20
Height of lower attach. B from ground [m]	h_2	4.38	0.88

Angle of Leg to Ground (static case) [°]	Beta_0	32.6	32.6
Angle of Strut to Ground (static case) [°]	Beta_1	52.3	52.3
Leg Length [m]	[PB]	8.13	1.62
Strut Length [m]	[PT/KP]	11.2/7.62	2.24/1.52
Mass LL [kg]	-	n.a.*	8.6
Absorber [kg]	-		37.9
Test rig [kg]	-		209

*the mass for the LL in 1:1 confg. is not available because no final 1:1 model was in the scope of the RETALT programme

Table 2-1: Geometry of the LL in deployed configuration

For the test breadboard a few simplifications and modifications between the 1:1 full scale design and the 1:5 test breadboard were made because of cost saving reasons. The design comparison between 1:1 and 1:5 is shown in Figure 2-2. E.g. the bridge (see also Figure 2-4) was designed as plane rod instead of a curved geometry, which is able to cover the absorber in folded configuration during flight. This has negligible impact on the structural behaviour of the LL.

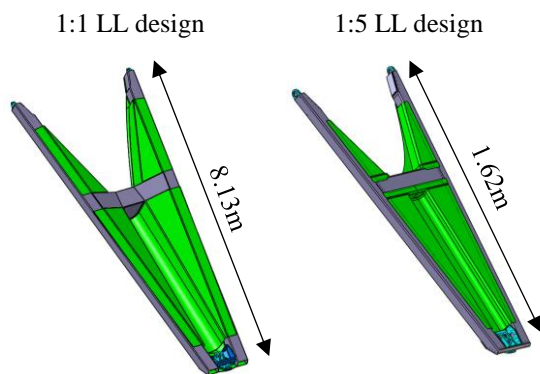1:1 LL design   1:5 LL design

8.13m   1.62m

Figure 2-2: Geometry comparison between 1:1 and 1:5 LL

As mentioned above the scaling 1:5 relates only to the geometry. For the mass, the scaling of 5 is not applicable. The scaling of mass increases cubically and cannot be directly applied on the CFRP. The exact mass of the 1:1 LL needs further investigations and strength analysis and was not the task in the RETALT programme.

The complete test setup including LL, absorber, absorber rod end and test rig is shown in

(1) LL (CFRP), (2) Absorber, (3) Absorber rod, (4) Test rig

Figure 2-3: Test setup for the landing leg.
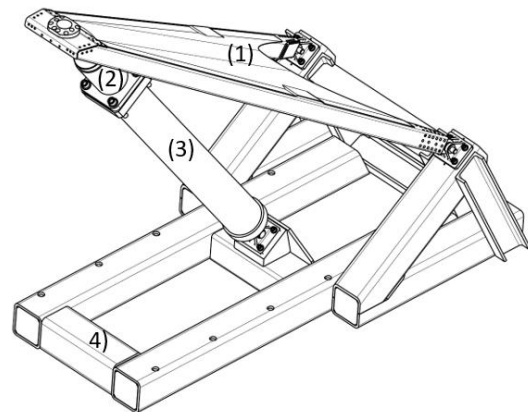
(1) LL (CFRP), (2) Absorber, (3) Absorber rod, (4) Test rig

Figure 2-3: Test setup for the landing leg

2.2 Description of the components of the test setup

The tasks of main components of the test setup are explained in the following bullet points:

- Bridge: increase stiffness against buckling and bending effects during landing
- Beams: sustain tension, bending and torsion loading during landing
- Absorber: dissipating kinetic energy during touch down
- Test rig: stiff fixation to test field

It has to be mentioned, that the test setup did not include the absorber bay and aerodynamic covers on the main frame during the test. This would have prevented the accessibility of the ARAMIS measurement (see chapter 3.5) on the load carrying structure.

2.3 Materials

The main structures such as beams, bridge and covers are made of CFRP (Prepreg). Metallic components are made of 3D printed Ti-6-4 or 1.4301 base sheet metal. A detailed description of the materials and the corresponding components are listed in [2].
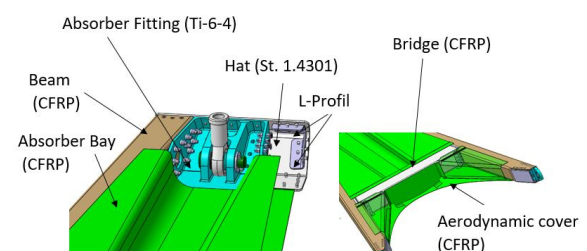
Absorber Fitting (Ti-6-4)   Bridge (CFRP)

Beam (CFRP)   Hat (St. 1.4301)   L-Profil

Absorber Bay (CFRP)

Aerodynamic cover (CFRP)

Figure 2-4: Components and corresponding materials

3   DEFINITION OF TEST AND TEST RESULTS

The chapter on hand gives on overview of the general objectives of the test, scope and applicability, verification of requirements, test conditions, instrumentation, test facility, test sequence, pass and fail criteria of the test and the test results.

3.1 General objectives

The main objectives in the test campaign were defined as follows:

- Applying the total kinetic energy to reach the max. predicted force of approx. 80KN
- Execution of the test matrix (Table 3-1)
- Measurement of strains and the kinematics of the landing leg respectively the absorber
- Exclusion of damage of the structure
- Evaluation of test results corresponding to test prediction

3.2 Scope and applicability

This impact test aims to verify the capability of the LL to withstand the specified kinetic energy and the corresponding forces, as well as to demonstrate and assess the quality of the manufactured structures. Furthermore, in course of the post-test activities, the test results will also serve to:

- verify the numerical analysis i.e. the Multi Body Dynamics (MBD) and Finite Element Method (FEM) model including assumed material properties and to adapt the modelling accordingly, if necessary
- determine the actual material properties in order to enable refinement of the numerical models

3.3 Requirements to be verified

For the impact test no detailed requirements are specified in the generic specification of the RETALT project of reusable launchers [1] e.g. specific energy, maximum force or environmental conditions such as temperature. Therefore, no hard requirement had to be verified. Nevertheless, general requirements were assumed, which requirements are based on the MTA experience of testing of comparable spacecraft components. Therefore, the kinetic energy and the corresponding force was defined by MTA as key requirement. It is adapted to the geometry of the 1:5 scaled LL and the corresponding highest mechanical load capacity for a standard rod end, available for aerospace applications. It has to be mentioned, that the first approach to specify the max. force for the test was a linear scaling of mass from the 1:1 launcher configuration down to 1:5. This mass

scaling led to a very low kinetic energy definition, which has to be dissipated. The corresponding low drop height to target the low defined kinetic energy did not result in a representative kinematic behaviour of the landing gear. Therefore, it was decided to proof the possible highest force, limited by geometric restrictions in the absorber fitting (see Figure 2-4).

3.4 Test conditions

The test was performed at ambient condition.

3.5 Instrumentation

The instrumentation was realized by strain gauges applied on the highest loaded regions and in regions with low stress gradients (see Figure 3-1) determined by FEM simulation.
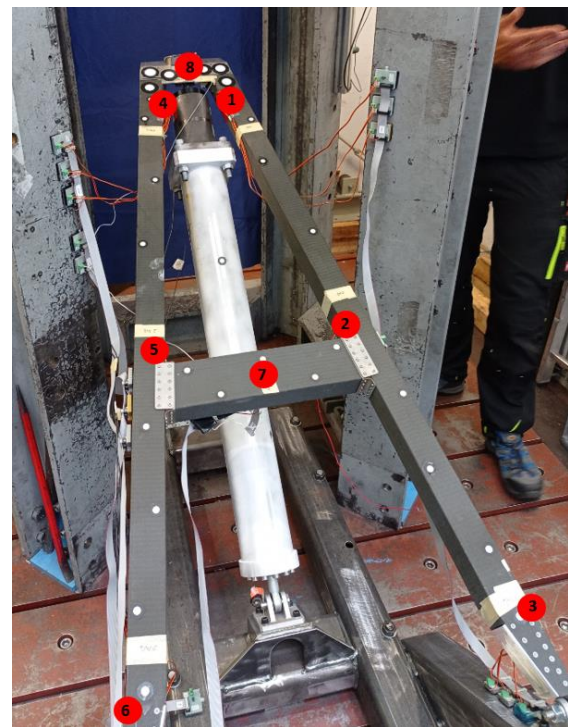

Figure 3-1: Position of 8 strain gauges numbering on the LL

Additional to the optical measurement system ARAMIS (see Figure 3-3), two accelerometers between the absorber piston and the fixed end (see figure 3-2) were applied.
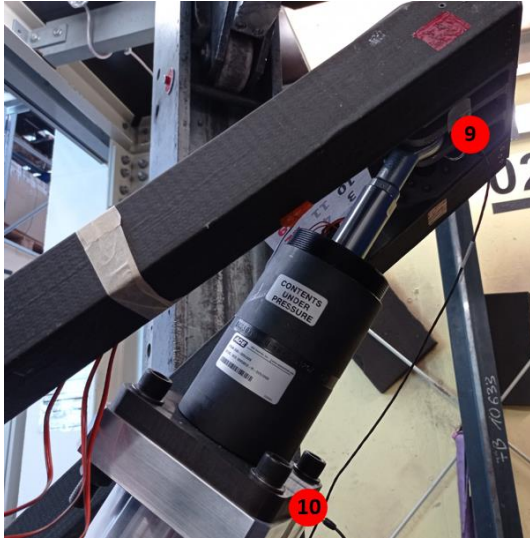
Figure 3-2: Position of accelerometers 1 & 2

The optical measurement system consists of high-speed cameras and the software, which visualizes the observed displacements over time. To track the structure, the components were marked with reference points, realized by small patches (see Figure 3-3).
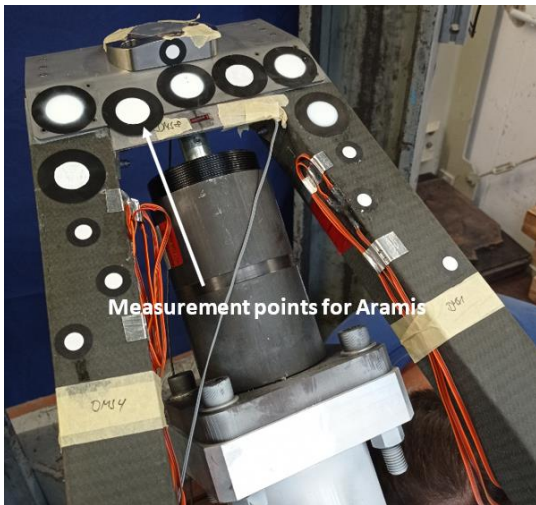

Figure 3-3: Measurement points of the optical measurement system ARAMIS

The optical instrumentation via ARAMIS is defined aiming to enable the comparison with the dynamic analysis of the MBD mathematical model results and the FEM model.

3.6 Test facility
The test was performed at LZS, Dresden, Germany using the impact test tower with a maximum height of approx. 24m and a max. applicable mass of approx.1200kg. This corresponds to max. energy

capacity of 283kJ. The test setup was delivered in assembled condition to the LZS test facility and was installed on the test field. The test field consists of a massive concrete block, mounted on springs to decouple it from external vibrations. The centred drop mass is guided along guiding steel rails and impacted the touch pad vertically. Lateral forces are not introduced by the impact mass. The test setup is shown in Figure 3-4.
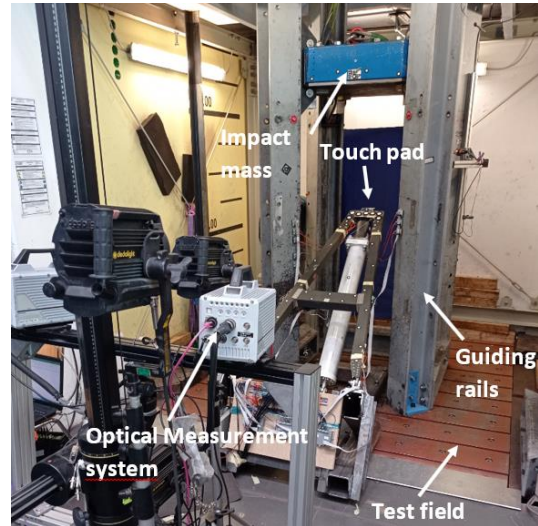

Figure 3-4: Test facility and setup

3.7 Test sequence
The test procedure is divided into four main sections. The first test section is the pre-test (I), the so-called calibration test. Within this pre-test the measured strains are correlated with the applied weight under quasi static loading to derive the force distribution in the leg and the damper. The reaction forces in the LL were calculated by bar structure mechanics formulas and the corresponding angles were measured by a digital angle meter. Correlating the measured values from the subsequent dynamic test with the quasi static loading (QSL) measurement from (I), the reaction forces can be derived indirectly for the dynamic test. A direct measurement system such as a load cell could not be installed because of limited available space. The second test section (II) is a shock test w.o. the absorber. The third (III) and fourth (IV) dynamic test section are identical in impact mass but differ in impact velocity, realized by a different drop height and they differ in the reduction of the stroke length of the absorber. The (III) section guarantees a stroke of 40mm and the (IV) 50mm.

During the (III) section, an additional test run with higher friction coefficient (approx. 0.5), realized by rubber patch at the touch pad, was included. The

intention of this additional run was to determine the impact of friction on the reaction forces in the LL.

The applied test matrix is shown in Table 3-1.

No.	Descript.	Drop height [m]	Drop mass [kg]	Drop vel. [m/s]
1	Static load (I)		365.5	
2		-	488.5	-
3			608.5	
4			365.5	
5	Shock test (II)	0.03	365.5	0.77
6	Impact test (III) (nominal friction)	0.1	365.5	1.4
7		0.3		2.43
8		0.5		3.13
9		0.3		2.43
10	Impact test (high friction)	0.1	365.5	1.4
11	Impact test (IV) (nominal friction)	0.1	365.5	1.4
12		0.5		3.13
13		0.7		3.71
14		0.9		4.2
15		0.5		3.13
16		0.9		4.2

Table 3-1: Test sequence applied at LZS

3.8 Pass/ fail criteria

The tests are considered successful, if:

- the defined kinetic energy is applied
- the defined max. reaction forces are reached
- No visual damage is detected after the test run
- No significant change between two (not consecutive) test runs with identical load level (so called pre- and post runs, e.g. Table 3-1 run 7 and 9)

3.9 Test results

The test results chapter is divided into four sections, which cover the 3 types of instrumentation, which are described in chapter 3.5. and a first assessment via FEM. For this paper it has to be mentioned, that the results are a preliminary and a rough evaluation, since the postprocessing, due to the large amount of recorded data, is still ongoing. Only the run no. 5 (Table 3-1) was evaluated. For the shock test (no. 5), the absorber behaved as a stiff rod w.o. its damping properties resulting from the viscosity of the fluid. This was an additional outstanding test procedure and serves as a first assessment of the deformations and strain characteristics of the LL.

3.9.1 Strain gauge measurement

This chapter gives a first overview of the strain measurements during the test campaign no. 5 (see Table 3-1). In Figure 3-5 all DMS are operating properly, which corresponds to a measurement output of 21 channels. The maximum measured strain of 0.13% occurred at pos. 1 (see Figure 3-1) in fibre direction. At the opposite side at pos. 4 the

strain shows a similar value of about 0.125% and shows a similar stiffness representation in this region. The DMS 8 shows a negative strain value of approx. -0.067%, which is also in line with expected behaviour.
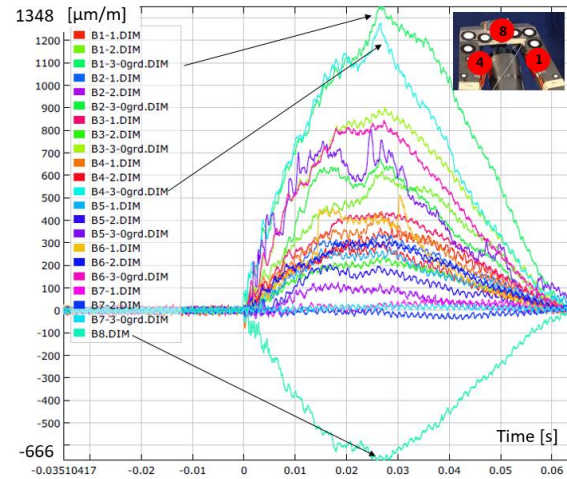

Figure 3-5: Strain measurements at critical locations

Further investigations are ongoing and need additional investigation to make a profound conclusion.

3.9.2 Optical measurement (ARAMIS)

The measurement points (see Figure 3-3) provide the displacement, velocity and acceleration during the impact test by the ARAMIS system. In Figure 3-6 the displacements of a first assessment for the displacements in axial y-direction are illustrated. The red arrows in Region I show the largest displacements at the end of LL, which represents the expected behaviour, confirming the prediction. In Region II displacements in y-direction occurred during the test, which is not in line with prediction. The Region II was assumed fixed in y-direction. This effect can be explained by the movement of the whole test field depending on its mounting, described in chapter 3.6. For the evaluation this translational displacement has to be considered for the displacement determination of the LL.

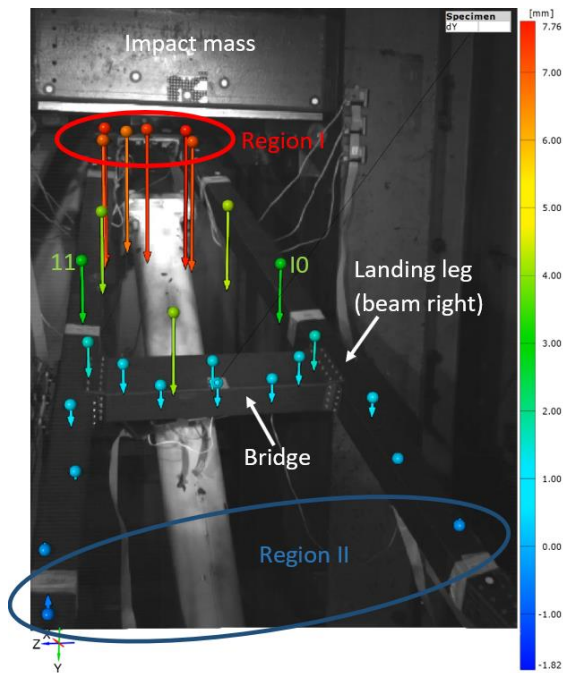#### 3.9.3 Measurement by accelerometer
Pending test evaluation

Figure 3-6: Measured displacement in y- direction on the LL via the optical measurement system ARAMIS

In general, the deformation of the LL under central loading was uniform between the right and left beam, comparing the measurement points e.g. point 10 and 11 see Figure 3-6.

3.9.4 First strain comparison between FEM and test results

A first comparison of strains between test and FEM simulation is made in this paper to assess qualitatively the strain distribution in the beams. The simulated strain unter static loading in fibre direction over the whole beam is shown in Figure 3-7.
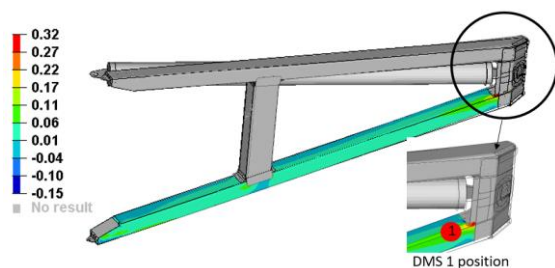

Figure 3-7: Strain in fibre direction in beam right under max. specified static loading

The DMS 1 shows in the simulation the largest value over the whole beam, such as the measured strain gauge B1-3 in fibre direction in Figure 3-5 does. Thus, the trend for the maximum of measured strain is in line with the prediction.

3.9.5 First displacement comparison between FEM and test results

Such as for the strains, first comparison of displacements between test and FEM simulation is illustrated in this paper to assess the qualitatively displacement distribution in the LL. The simulated displacements in y-direction under static loading are shown in Figure 3-8. The simulation shows a similar trend compared to the test results. The max. measured displacements at the end of the LL are also determined in the FEM. The largest discrepancy between between test and simulation is in the region of fixation, where the displacements should be zero. This was not observed in the test and needs further investigation. A first assessemnt concerning this issue is exaplained in chapter 3.9.2.
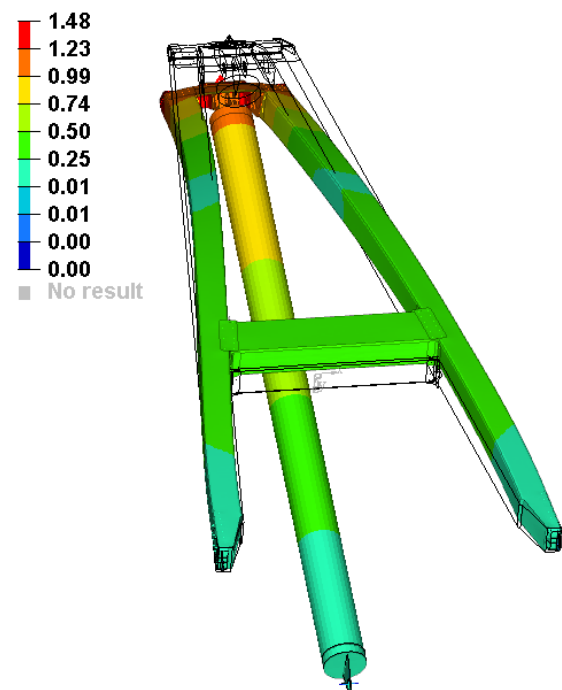

Figure 3-8: Displacement under max. specified static loading (amplified by a factor of 10)

4 AERODYNAMIC CONTROL SURFACES

The application of the aerodynamic control surfaces (ACS) is at the top of the core stage shown in Figure 4-1 and serves to control the launcher during descend flight.
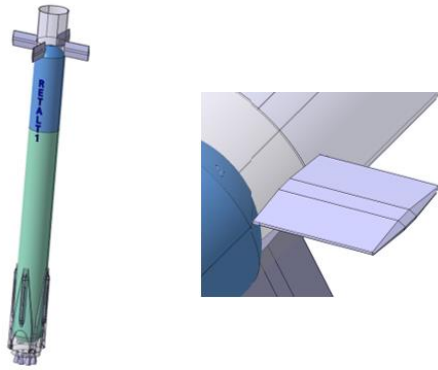
Figure 4-1: Application of ACS at the launcher [4]

The ACS is represented in Figure 4-2 and shows a control surface including internal stiffener made of CFRP and titanium. The structure of the fin itself can be seen as state of the art, in terms of manufacturing of the metallic and composite components. The intended titanium root fitting, however, represents an increased degree of complexity. MT Aerospace will consider the viability of producing the part using metallic additive manufacture.
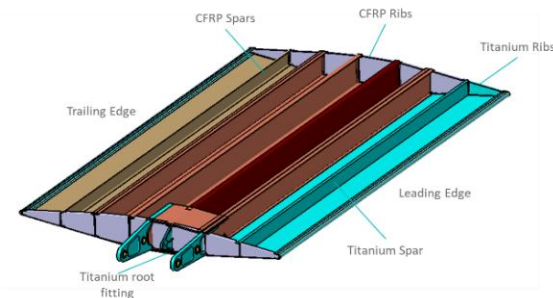

Figure 4-2: Overview of control surface

The final scaled manufactured ACS is shown in Figure 4-3. The complex root fitting is conventionally manufactured by milling for the demonstrator and made of aluminium. Further details for the ACS and shown in [3].

Figure 4-3: Final scaled control surface

5   CONCLUSION AND FUTURE WORK

It can be concluded, that the main objectives of the testing programme (chapter 3.1) were successfully fulfilled. The max. kinetic energy was reached and the integrity of the structure was judged intact by visual inspection. NDI such as ultra-sonic inspection was not foreseen in this project. The test was monitored sufficiently by conventional strain gauges and accelerometers and the optical measurement systems and were used for a first assessment between the numerical simulation and test data shown in chapter 3.9.4.

The tested 1:5 LL has proven to be a key element for future reusable launcher for European space programmes.

The future work is to manufacture a 1:1 landing leg and test it in relevant environmental conditions to reach the next TRL level 5.
Another key point is the correlation of the recorded data of the 1:5 scaled LL during the test with the mathematical models available. The correlation and adaption e.g. material properties of the mathematical is the basis to transfer the knowledge e.g. mechanical behaviour or kinematic behaviour from the 1:5 to the 1:1 configuration.

6   ACKNOWLEDGEMENT

7   REFERENCES

[1] Marwege, A., Klevanski J., Riehmer J.: System Definition Report (2022)

[2] Thies, C.: D5.15 Landing leg demonstrator in representative scale incl. (2022)

[3] Jevons, M., Starke P.: D5.6_Fin Manufacturing Model Delivery Report (2021)

[4] Marwege, A.; Gülhan, A.; Klevanski, J.; Riehmer, J.; Kirchheck, D.; Karl, S.; Bonetti, D.; Vos, J.; Jevons, M.; Krammer, A.; Carvalho, J.: „Retro Propulsion Assisted Landing Technologies (RETALT): Current Status and Outlook of the EU Funded Project on Reusable Launch Vehicles", 70th International Astronautical Congress (IAC), Washington D.C., United States, 21-25 October 2019.